The expression analysis of mouse interleukin-6 splice variants argued against their biological relevance

Giosuè Annibalini[*]*, Michele Guescini, Deborah Agostini, Rita De Matteis, Piero Sestili, Pasquale Tibollo, Michela Mantuano, Chiara Martinelli & Vilberto Stocchi*

Dipartimento di Scienze Biomolecolari, Università degli Studi di Urbino "Carlo Bo", via I. Maggetti 26, 61029 Urbino (PU), Italy

Alternative splicing generates several interleukin-6 (IL-6) isoforms; for them an antagonistic activity to the wild-type IL-6 has been proposed. In this study we quantified the relative abundance of IL-6 mRNA isoforms in a panel of mouse tissues and in C2C12 cells during myoblast differentiation or after treatment with the Ca^{2+} ionophore A23187, the AMP-mimetic AICAR and TNF-α. The two mouse IL-6 isoforms identified, IL-6δ5 (deletion of the first 58 bp of exon 5) and IL-6δ3 (lacking exon 3), were not conserved in rat and human, did not exhibit tissue specific regulation, were expressed at low levels and their abundance closely correlated to that of full-length IL-6. Species-specific features of the IL-6 sequence, such as the presence of competitive 3' acceptor site in exon 5 and insertion of retrotransposable elements in intron 3, could explain the production of IL-6δ5 and IL-6δ3. Our results argued against biological significance for mouse IL-6 isoforms. [BMB reports 2012; 45(1): 32-37]

INTRODUCTION

Cytokines as hormones play a fundamental role in the communication between cells, even if they act at a lower concentration (nano-picomolar) and are not stored in glands but are rapidly synthesized and secreted, mostly after specific stimuli.

Interleukin-6 (IL-6) belongs to the family of cytokines which is characterized by the long-chain α-helix-bundle topology and by the use of gp130 as a common signal transducer. IL-6 plays a central role in the inflammatory response and its aberrant production has been implicated in several diseases, including many types of cancer (1). Human, mouse and rat IL-6 gene is structured in 5 exons and 4 introns. The position of exon/intron junctions, the length of exons, and the position of cysteine residues within the IL-6 sequence are conserved in different mammalian species (2).

Several alternative splicing (AS) variants of IL-6 gene have been identified in human and mouse. In human, in addition to full-length (FL) IL-6, an isoform lacking exon 2 (IL-6δ2) has been identified in lipopolysaccharide-stimulated peripheral blood mononuclear cells (PBMC) (3), in normal renal cells and renal cell carcinoma (RCC) but not in other tumour cells (4). In lung tissue and cultivated fibroblasts, in addition to FL IL-6 and IL-6δ2, also IL-6 lacking exon 4 (IL-6δ4) and both exon 2 and 4 (IL-6δ2δ4) have been reported (5). Two other IL-6 isoforms, involving different exons compared to human ones, were found in mice (6). FL IL-6, IL-6δ5 (deletion of the first 58 bp of exon 5) and IL-6δ3 (lacking exon 3) were expressed in the spleen of mice previously immunized with sheep erythrocytes and in placenta tissues, whereas only FL IL-6 and IL-6δ5 have been detected in liver (6). In man, functions of IL-6 isoforms have been analysed using an *in vitro* translation assay of IL-6 cDNA splice variants. IL-6δ4 (5) and IL-6δ2 (4), expressed as recombinant proteins, revealed an antagonistic activity to the wild-type IL-6. More recently, a bioinformatic analysis of human IL-6δ2, IL-6δ4 and mouse IL-6δ3 structures and their modelled interactions with the receptor complex suggested that all these splice variants could act as antagonists of IL-6 (7). All these studies showed that multiple mRNAs of IL-6 are produced and, if translated, they could regulate the activity of wild-type IL-6. An antagonistic action of IL-6 isoforms requires that IL-6 isoforms are expressed in relatively high level compared to FL IL-6. However, to date, no study has analysed the relative abundance of IL-6 isoforms compared to FL IL-6 and if their ratio of expression is regulated. In this study we quantified the relative abundance of IL-6 mRNA isoforms in a panel of normal mouse tissues using real time RT-PCR. Moreover, we used the murine C2C12 cells to investigate if the expression of IL-6 mRNA isoforms was dynamically controlled during myoblast differentiation and after several stimuli known to induce IL-6 expression through the activation of different pathways (8). Finally we described the pattern of expression of IL-6 splice variants in several rat tissues and human normal and tumour cell lines in order to analyse if mouse IL-6 isoforms are conserved among closely related species.

RESULTS AND DISCUSSION

Identification and quantification of IL-6 isoforms in a panel of mouse tissues

Expression of IL-6 splice variants in mouse tissues was analysed by RT-PCR using primers located at the extreme 5′ and 3′ ends of the coding sequence. A PCR product of the expected size for IL-6 (640 bp) was amplified in lung, intestine, skeletal muscles (gastrocnemius and soleus), adipose tissues (inguinal and mesenteric) and heart of mice; two other fragments of smaller length were also present in lung and mesenteric adipose tissue (Fig. 1A). Sequence analysis showed that the band of 640 bp corresponds to FL IL-6 whereas the two lower bands obtained in lung and mesenteric adipose tissue correspond to the same IL-6 isoforms previously described in mice (6): IL-6δ5 (582 bp) and IL-6δ3 (526 bp).

We then quantified the relative abundance of IL-6 splice variants by using real time RT-PCR. Fig. 1B shows the IL-6 exon/intron structure and the position of primers used for the amplification of FL IL-6, IL-6δ5 and IL-6δ3. Among all the tissues examined, mesenteric adipose tissue expressed the high-

est level of FL IL-6 mRNA, followed by lung, skeletal muscles, heart and inguinal adipose tissue (Fig. 1C). In brain and intestine FL IL-6 was barely detectable whereas liver and kidney do not express FL IL-6 at all. Using real time RT-PCR we detected IL-6δ5 and IL-6δ3 not only in lung and mesenteric adipose tissues as obtained with conventional PCR, but in all tissues expressing FL IL-6. This result demonstrated that IL-6δ5 and IL-6δ3 were expressed without tissue-selectivity but their detection was related to the sensitivity of the experimental method. Quantification of IL-6 isoforms by real time RT-PCR revealed that FL IL-6 accounted for over 90% of total IL-6 mRNAs whereas IL-6δ5 and IL-6δ3 represented 5-6% and 3% respectively.

There was a close correlation between the expression of FL IL-6 and IL-6δ5 (r = 0.9; P < 0.01) and IL-6δ3 (r = 0.9; P < 0.01) although their quantity was too low to suggest regulatory functions for these AS variants.

Analysis of IL-6 splice variants in C2C12 cells

After that, we analysed the expression of IL-6 isoforms in murine C2C12 cells, since numerous studies have shown that skeletal muscle cells express IL-6 and its mRNA abundance is regulated during differentiation of myoblasts to myotubes (9) and to several stimuli including inflammatory mediators (10), rise in intracellular Ca^{2+} concentration and activation of the fuel-sensing enzyme AMPK (11). With PCR primers flanking the sequence of the IL-6 coding region, FL IL-6, IL-6δ5 and IL-6δ3 were amplified both in myoblasts and myotubes (Fig. 2A). Quantification of IL-6 isoforms by real time RT-PCR revealed that in C2C12 the expression level of IL-6δ5 and IL-6δ3 was low indeed, together, they never reached more than 10% of total IL-6 mRNAs (Fig. 2B). These data were consistent with those obtained in mouse tissues. Myotubes expressed about twice the FL IL-6, IL-6δ5 and IL-6δ3 than the myoblasts and about 10 fold more IL-6 isoforms compared to skeletal muscle *in vivo* (compare Fig. 1C and 2B). This marked difference between the expression of IL-6 in cell cultures versus isolated tissues has been previously described (12) and may be related to the differentiation state or to autocrine stimulation of IL-6 production. This finding explains why IL-6δ5 and IL-6δ3 were detected, by RT-PCR, in C2C12 cells but not in mouse skeletal muscles.

To determine whether the IL-6 isoforms are efficiently exported in the cytoplasm, we quantified the relative abundance of IL-6 mRNA isoforms in nuclear and cytoplasmic fractions of myotubes. The FL IL-6 and IL-6δ5 were nearly equally expressed in the nucleus and cytoplasm while IL-6δ3 was partially retained in the nucleus demonstrating that this AS variant, as many miss-spliced mRNAs (13), was inefficiently exported to the cytoplasm to prevent protein expression (Fig. 2C). The cytoplasmic proteins Gapdh and Tubulin were used to confirm the purity of nuclear fraction (Fig. 2D).
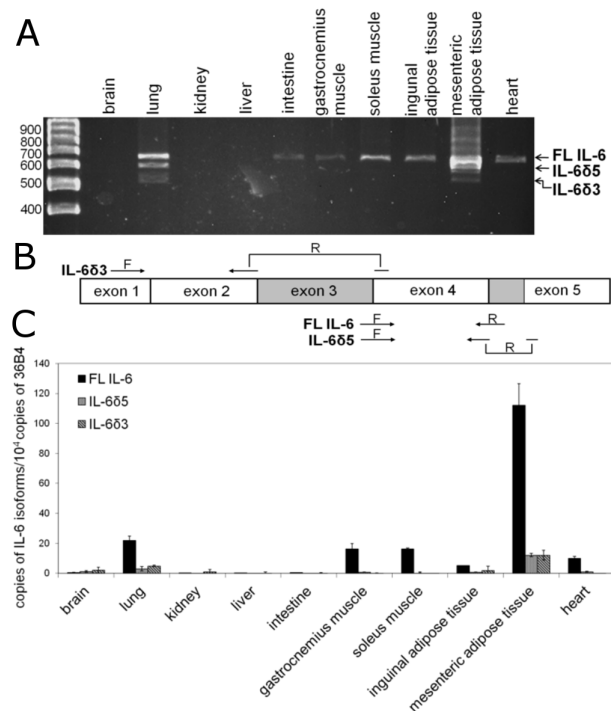

Fig. 1. Expression analysis of IL-6 isoforms in a panel of mouse tissues. (A) IL-6 mRNAs expressed in several mouse tissues were amplified using primers located at the 5′ and 3′ ends of the coding sequence. (B) Schematic representation of the exon/intron structure of IL-6 gene and position of primers used to separately amplify IL-6 isoforms. The alternative exon 3 and the sequence removed from IL-6δ5 are shown in grey. (C) Quantification of IL-6 isoforms by real time RT-PCR in mouse tissues.
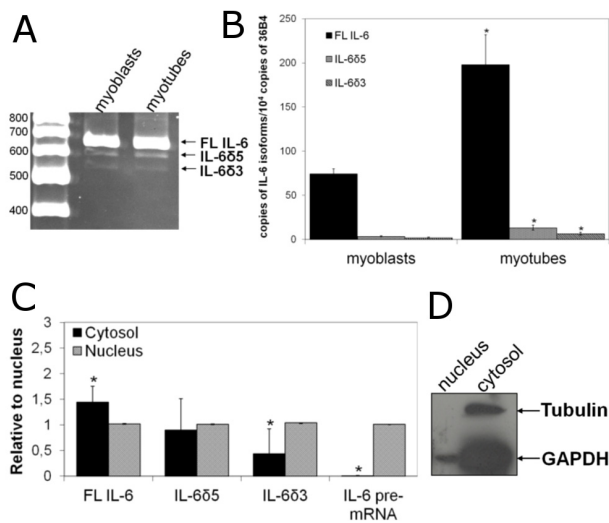
Fig. 2. Expression analysis of IL-6 splice variants in C2C12 myoblasts and myotubes. (A) RT-PCR amplification pattern obtained in C2C12 myoblasts and myotubes with primers located at the 5′ and 3′ ends of the coding sequence and (B) quantification of IL-6 isoforms by real time RT-PCR (n = 7 *P < 0.05). (C) Quantification of IL-6 isoforms in nuclear and cytoplasmic fractions of myotubes (n = 3 *P < 0.05); the cytoplasmic fraction is virtually free of nuclear contamination as assessed by IL-6 pre- mRNA expression. (D) The cytoplasmic proteins Gapdh and Tubulin were predominantly found in the cytosol fraction confirming the purity of nuclear fraction.

Fig. 3. Real-time RT-PCR measurements of IL-6 isoforms during myoblast differentiation and after different C2C12 treatments. (A) Quantification of IL-6 isoforms during C2C12 differentiation (n = 3 *P < 0.05). Quantification of IL-6 isoforms in myotubes treated for: (B) 16 h with the AMP-analog AICAR (0.1, 0.5 and 1 mM); (C) 6 h with pro-inflammatory cytokine TNF-α (10, 20 and 50 ng/ml); and (D) 16 h with the Ca^{2+} ionophore A23187 (0.1, 0.5 and 1 μM) (n = 3 *P < 0.05).

much stronger compared to AICAR and TNF-α, and this effect was seen only in myotubes. These results confirmed recent studies which demonstrated that Ca^{2+} plays an important role in muscle IL-6 production (11).

Quantification of IL-6 isoforms during myoblast differentiation and after different C2C12 treatments

Since the expression of IL-6 isoforms markedly differs between myoblasts and myotubes, we analysed the pattern of expression of FL-6, IL-6δ5 and IL-6δ3 during C2C12 differentiation. FL IL-6 expression was low in proliferative myoblasts (60-70% confluence) and slightly increased when cells reached 100% confluence and 24 hours after the initiation of differentiation induced by serum withdrawal (T1). On the second day (T2) of myoblast differentiation, FL IL-6 mRNA was strongly upregulated, reaching its peak of expression, and then declining at T3 and T4 when myotubes were fully differentiated (Fig. 3A). This result is consistent with previously published data showing a promyogenic role of IL-6 (14). During C2C12 differentiation, the level of IL-6δ5 and IL-6δ3 was lower than the level of FL IL-6, and, as already obtained in mouse tissues, their pattern of expression strictly correlated to that of FL IL-6 (r = 0.9; P < 0.01). The close correlation between the expression level of FL IL-6 and IL-6δ5 and IL-6δ3 was also demonstrated by treatment of C2C12 with the AMP-analog AICAR, the pro-inflammatory cytokine TNF-α and the Ca^{2+} ionophore A23187 (Fig. 3B-D respectively). All these treatments induced a dose-dependent expression of IL-6 isoforms in myoblasts (not shown) and myotubes, even if the quantity of IL-6δ5 and IL-6δ3 was negligible compared to FL IL-6. Interestingly, the upregulation of FL IL-6 mRNA after the A23187 treatment was
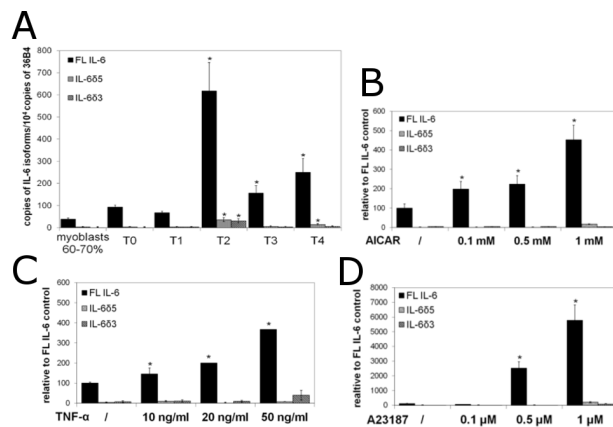
Analysis of IL-6 isoforms expression in rats and humans

Using the Unigene database (www.ncbi.nlm.nih.gov/UniGene) we analysed the IL-6 isoforms conservation between mammalian species. In human 102 cDNA correspond to FL IL-6; 2 to IL-6δ2 (CD013918.1; AA381568.1) and one to IL-6 with partial deletion (69 bp) of exon 2 (BE787841.1). In mouse 14 sequence correspond to FL IL-6 and one to IL-6δ5 (BC145409). In pig, cow and rat 16, 14 and 5 sequences respectively correspond to FL IL-6 while no IL-6 isoform was found. The species- specific production of mouse, rat and human IL-6 isoforms was also confirmed by canonical RT-PCR. We analysed the IL-6 isoforms in rat skeletal muscles (gastrocnemius and soleus), adipose tissues (mesenteric and inguinal) and liver amplifying a single PCR product corresponding to FL IL-6 in soleus muscle and mesenteric adipose tissue (Fig. 4A). In order to exclude the presence of low expressed rat IL-6 isoforms we reamplified with nested primers the amplicons of previous PCR obtaining a single PCR product (FL IL-6) in all tissues (Fig. 4B). In all human cells analysed (PBMC, skeletal muscle, HeLa, U87 and HUVEC), in addition to FL IL-6 (568 bp), we amplified also a lower PCR band corresponding to IL-6 missing exon 2 (IL-6δ2; 377bp) (Fig. 4C). This analysis showed that IL-6δ2 isoform expression was not associated with specific cell lineages as previously suggested (4); further studies are needed to quantify the relative abundance of this AS variant and hence clarify its functional relevance. Notably IL-6δ5 and IL-6δ3 have
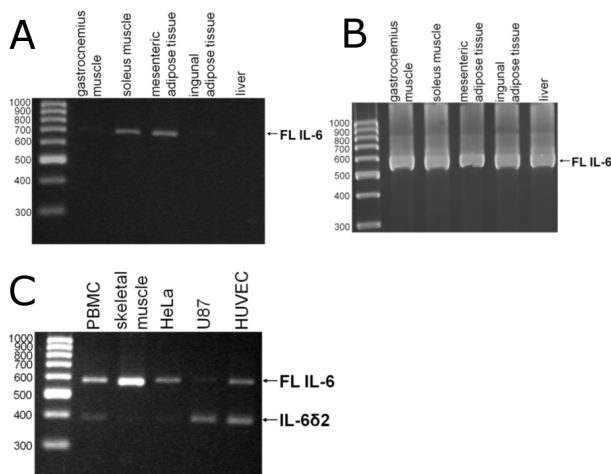
Fig. 4. Identification of IL-6 mRNA isoforms in rat and human. (A) RT-PCR amplification pattern obtained in several rat tissues. (B) Reamplification with nested primers of PCR amplicons showed in (A). (C) RT-PCR analysis of IL-6 transcripts in several normal and cancer cell lines.

not been identified in any others species than mouse.

Analysis of mouse IL-6 sequence and its splice sites features

What are the specific features of mouse IL-6 sequence that induce the (low) production of IL-6δ5 and IL-6δ3? The alternative 3' acceptor site used in mouse IL-6δ5, not conserved in rat and human gene, has a lower strength (Max Entropy (ME) = 9.16), higher exonic splicing enhancers (ESE) density (2.18) and lower intronic splicing regulator (ISR) density (0.6) compared to that of intron4/exon5 boundary of FL IL-6 (ME = 12.40; ESE density = 0.7; ISR = 1.38) (15). All these features may therefore explain the greater use of the canonical 3' acceptor site of FL IL-6 compared to the nearby "competing" alternative 3' acceptor site of IL-6δ5 (16).

Mouse IL-6 sequence shows also a species-specific feature that may explain IL-6δ3 production. Indeed multiple alignments of mouse, rat and human IL-6 sequence revealed that mouse intron 3 contains a long interspersed nuclear element 1 (LINE-1) of 1956 bp and a B2 short interspersed nuclear element (B2-SINE) of 198. Many studies have shown that insertion of LINE-1 into the intron of a gene causes exon skipping (17, 18), therefore the species-specific production of IL-6δ3 isoform is likely to be explained by the introduction of a retrotransposon in mouse intron 3.

Recent studies have demonstrated that nearly every multi-exon gene, including "constitutively" spliced genes (19), produces alternative mRNA isoforms (20). Although many of these isoforms have important functional roles, it is clear that some of these mRNAs are produced by errors during the splicing process (21). In fact, different RNA quality controls have evolved to find and degrade the errors that do occur and anyway, if expressed at low levels, the new mRNA isoforms could be tol-

erated by the cell and eventually represent an evolutionary precursor (22). It is difficult to prove that a transcript does not have any function in any tissues or in different physiological or pathological conditions, especially for pleiotropic genes like IL-6. Anyway, in the present study, analysing different tissues and cell culture treated with several stimuli, we demonstrated a relative low abundance of IL-6δ5 and IL-6δ3, a close correlation to FL IL-6 and specie-specific production of IL-6 isoforms. Expression of IL-6δ5 and IL-6δ3 is probably related to unique features of mouse IL-6 sequence and these isoforms are likely to be the result of errors in the splicing process.

MATERIALS AND METHODS

Cell lines and tissues

C2C12 were purchased from Istituto Zooprofilattico Sperimentale (Brescia, Italy); HeLa, U87 and Human Umbilical Vein Endothelial Cells (HUVEC) were obtained from Banca Biologica and Cell Factory (Genova, Italy). Human Skeletal Muscle RNA (Cat# 7982) was purchased from Ambion (Milan, Italy); PBMC were isolated from a healthy donor (male, aged 60) by density gradient centrifugation (Lymphoprep, Celbio, Italy).

Four-month old female BALB/c mice (n = 3) (Harlan, Italy) and Young Sprague Dawley male rat (10-week old; n = 3) were housed with a 12-h light/dark cycle and free access to standard laboratory chow and water. Care and handling were in accordance with institutional and national guidelines. Animals were sacrificed with an overdose of anaesthetics (ketamine in combination with xylazine). All tissues were immediately dissected out, immersed in RNAlater and homogenized using a rotor-stator homogenizer and then stored at −80°C before RNA extraction.

Cell culture

The murine C2C12 cells were cultured as previously described (23). During C2C12 differentiation, cells were harvested by trypsinisation in proliferative phase (myoblasts 60-70% confluence), upon reaching confluence (T0) and in the following four days of differentiation (T1, T2, T3 and T4). For pharmacological treatments, confluent myoblasts and myotubes were incubated for 16 h with the AMP-analog AICAR (0.1, 0.5 and 1 mM) and the Ca^{2+} ionophore A23187 (0.1, 0.5 and 1 μM) and for 6 h with the pro-inflammatory cytokine TNF-α (10, 20 and 50 ng/ml).

RNA extraction and cDNA synthesis

Total RNA from C2C12 and mouse tissues was extracted and purified using an RNeasy kit (Qiagen GmbH, Hilden, Germany) according to the manufacturer's instructions. After DNA digestion with DNase I enzyme (Ambion, Austin, TX, USA) cDNA was synthesized from 1.5 μg of total RNA using Omniscript RT (Qiagen) and random hexamers.

Conventional RT-PCR

RT-PCR was performed in 50 μl of reaction volume with 4 μl of

cDNA, 800 nM of primers and 25 μl of 2X HotStartTaq mix (Qiagen). The primers used for RT-PCR were located at 5'- and 3'-end of IL-6 gene: MOUSE: forward 5'-CGCTATGAAGT TCCTCTCTGC-3' and reverse 5'-CTAGGTTTGCCGAGTAGAT CTC-3'; RAT: forward 5'-CCACCAGGAACGAAAGTCAA-3' and reverse 5'-GGTTTGCCGAGTAGACCTCATA-3'; HUMAN: forward 5'-CGGGAACGAAAGAGAAGCTC-3' and reverse 5'-AAC CACAAATGCCAGCCT-3'. RT-PCR conditions involved an initial denaturation step at 95°C for 10 min, followed by 35 cycles with denaturation step at 95°C for 30 sec, annealing at 60°C for 30 sec and extension at 72°C for 30 sec. PCR products were size-fractionated by electrophoresis on 4.0% agarose gels and visualized by ethidium bromide staining under UV light. Amplification products were purified with QIAquick gel extraction kit (Qiagen), cloned and sequenced.

Real time RT-PCR quantification of mouse IL-6 isoforms

Serial dilution (1 : 4) of three recombinant plasmids containing the FL IL-6, IL-6δ5 or IL-6δ3 isoforms and 36B4 were prepared in order to generate standard curves for plotting CT values against number of molecules. Molecules of each plasmid were calculated using the concentration of each plasmid, Avogadro's constant, the molecular weight of double-stranded DNA and the size of the target amplicon (24). The copy number of genes was calculated in individual samples using a corresponding reference plasmid cDNA clone at known concentration. The amount of target transcripts was shown as "copies of IL-6 isoforms/10^4 copies of 36B4". Percentage of IL-6 isoforms was calculated as [(mRNA of single isoform/(mRNAs of FL IL-6 + IL-6δ5 + IL-6δ3)×100]. The PCR was performed in a Bio- Rad iCycler iQ Multi-Coulor real time PCR Detection System using 2X Quantitect SYBR PCR kit (Qiagen) and 300 nM of each primer. The real-time PCR conditions were: 95°C for 10 min followed by 40 cycles of three-steps at 95°C for 30 sec, 60°C for 30 sec, and 72°C for 30 sec. The specificity of the amplification products was confirmed by examining thermal denaturation plots and by sample separation in a 4% DNA agarose gel. The following primers were used in real time RT-PCR quantification: FL IL-6: forward 5'-CTGGATATAATCA GGAAATTTGC-3' and reverse 5'-AAATCTTTTACCTCTTGG TTGA-3'; IL-6δ5: forward 5'-CTGGATATAATCAGGAAATTTG C-3' and reverse 5'-CTCCAGCTTATCTCTTGGTTGA-3'; IL-6δ3: forward 5'-CGCTA TGAAGTTCCTCTCTGC-3' and reverse 5'-GGCAAATTTCCTCT TTCTC-3'; 36B4 forward 5'-CGACCTGGAAGTCCAACTAC-3' and reverse 5'-ATCTGCTGCATCTGCTT G-3'.

The specificity of real time PCR primers was confirmed using three recombinant plasmids containing the complete sequences of FL IL-6, IL-6δ5 and IL-6δ3 as a template.

Isolation of cytoplasmic and nuclear RNA and proteins

Separation of cytoplasmic and nuclear fractions from myoblasts and myotubes was obtained as previously described (25). Efficient nuclear/cytoplasmic fractionation was assessed by Western Blotting with anti-Gapdh and anti-Tubulin anti-

bodies and by quantification of IL-6 pre-mRNA with primers flanking intron 1: forward 5'- CGCTATGAAGTTCCTCTCTGC -3' and reverse 5'-AACCCACAATGCTGGCTCT-3'.

Statistical analysis

The results are expressed as mean ± s.e.m. of the number of experiments indicated in the legend of each figure. The data were analysed by two-tailed t test, or ANOVA followed by Tukey's HSD test. $P < 0.05$ was considered significant difference.

REFERENCES

1. Hong, D. S., Angelo, L. S. and Kurzrock, R. (2007) Interleukin-6 and its receptor in cancer: implications for Translational Therapeutics. *Cancer* **110**, 1911-1928.
2. Simpson, R. J., Hammacher, A., Smith, D. K., Matthews, J. M. and Ward, L. D. (1997) Interleukin-6: structure-function relationships. *Protein Sci.* **6**, 929-955.
3. Kestler, D. P., Agarwal, S., Cobb, J., Goldstein, K. M. and Hall, R. E. (1995) Detection and analysis of an alternatively spliced isoform of interleukin-6 mRNA in peripheral blood mononuclear cells. *Blood* **86**, 4559-4567.
4. Alberti, L., Bachelot, T., Duc, A., Biota, C. and Blay, J. Y. (2005) A spliced isoform of interleukin 6 mRNA produced by renal cell carcinoma encodes for an interleukin 6 inhibitor. C*ancer Res.* **65**, 2-5.
5. Bihl, M. P., Heinimann, K., Rudiger, J. J., Eickelberg, O., Perruchoud, A. P., Tamm, M. and Roth, M. (2002) Identification of a novel IL-6 isoform binding to the endogenous IL-6 receptor. *Am. J. Respir. Cell. Mol. Biol.* **27**, 48-56.
6. Yatsenko, O. P., Filipenko, M. L., Khrapov, E. A., Voronina, E. N., Kozlov, V. A. and Sennikov, S. V. (2004) Alternative splicing of mRNA of mouse interleukin-4 and interleukin-6. *Cytokine* **28**, 190-196.
7. Denessiouk, K. A., Denesyuk, A. I. and Johnson, M. S. (2008) Negative modulation of signal transduction via interleukin splice variation. *Proteins* **71**, 751-770.
8. Pedersen, B. K. and Fischer, C. P. (2007) Physiological roles of muscle-derived interleukin-6 in response to exercise. *Curr. Opin. Clin. Nutr. Metab. Care.* **10**, 265-271.
9. Baeza-Raja, B. and Munoz-Canoves, P. (2004) p38 MAPK-induced nuclear factor-kappaB activity is required for skeletal muscle differentiation: role of interleukin-6. *Mol. Biol. Cell.* **15**, 2013-2026.
10. Al-Shanti, N., Saini, A., Faulkner, S. H. and Stewart, C. E. (2008) Beneficial synergistic interactions of TNF-alpha and IL-6 in C2 skeletal myoblasts--potential cross-talk with IGF system. *Growth Factors* **26**, 61-73.
11. Weigert, C., Dufer, M., Simon, P., Debre, E., Runge, H., Brodbeck, K., Haring, H. U. and Schleicher, E. D. (2007) Upregulation of IL-6 mRNA by IL-6 in skeletal muscle cells: role of IL-6 mRNA stabilization and Ca2+-dependent mechanisms. *Am. J. Physiol. Cell. Physiol.* **293**, C1139-1147.
12. Glund, S., Treebak, J. T., Long, Y. C., Barres, R., Viollet,

B., Wojtaszewski, J. F. and Zierath, J. R. (2009) Role of adenosine 5'-monophosphate-activated protein kinase in intreleukin-6 release from isolated mouse skeletal muscle. *Endocrinology* **150**, 600-606.

13. Dreyfuss, G., Kim, V. N. and Kataoka, N. (2002) Messenger-RNA-binding proteins and the messages they carry. *Nat. Rev. Mol. Cell. Biol.* **3**, 195-205.

14. Serrano, A. L., Baeza-Raja, B., Perdiguero, E., Jardi, M. and Munoz-Canoves, P. (2008) Interleukin-6 is an essential regulator of satellite cell-mediated skeletal muscle hypertrophy. *Cell. Metab.* **7**, 33-44.

15. Schwartz, S., Hall, E. and Ast, G. (2009) SROOGLE: webserver for integrative, user-friendly visualization of splicing signals. *Nucleic Acids Res.* **37**, W189-192.

16. Xia, H., Bi, J. and Li, Y. (2006) Identification of alternative 5'/3' splice sites based on the mechanism of splice site competition. *Nucleic Acids Res.* **34**, 6305-6313.

17. Meischl, C., Boer, M., Ahlin, A. and Roos, D. (2000) A new exon created by intronic insertion of a rearranged LINE-1 element as the cause of chronic granulomatous disease. *Eur. J. Hum. Genet.* **8**, 697-703.

18. Han, J. S. and Boeke, J. D. (2005) LINE-1 retrotransposons: modulators of quantity and quality of mammalian gene expression? *Bioessays* **27**, 775-784.

19. Fox-Walsh, K. L. and Hertel, K. J. (2009) Splice-site pairing

20. Pan, Q., Shai, O., Lee, L. J., Frey, B. J. and Blencowe, B. J. (2008) Deep surveying of alternative splicing complexity in the human transcriptome by high-throughput sequencing. *Nat. Genet.* **40**, 1413-1415.

21. Melamud, E. and Moult, J. (2009) Stochastic noise in splicing machinery. *Nucleic Acids Res.* **37**, 4873-4886.

22. Hsu, S. N. and Hertel, K. J. (2009) Spliceosomes walk the line: splicing errors and their impact on cellular function. *RNA Biol.* **6**, 526-530.

23. Sestili, P., Barbieri, E., Martinelli, C., Battistelli, M., Guescini, M., Vallorani, L., Casadei, L., D'Emilio, A., Falcieri, E., Piccoli, G., Agostini, D., Annibalini, G., Paolillo, M., Gioacchini, A. M. and Stocchi, V. (2009) Creatine supplementation prevents the inhibition of myogenic differentiation in oxidatively injured C2C12 murine myoblasts. *Mol. Nutr. Food. Res.* **53**, 1187-1204.

24. Overbergh, L., Valckx, D., Waer, M. and Mathieu, C. (1999) Quantification of murine cytokine mRNAs using real time quantitative reverse transcriptase PCR. *Cytokine.* **11**, 305-312.

25. Wang, Y., Zhu, W. and Levy, D. E. (2006) Nuclear and cytoplasmic mRNA quantification by SYBR green based real-time RT-PCR. *Methods* **39**, 356-362.

is an intrinsically high fidelity process. *Proc. Natl. Acad. Sci. U.S.A.* **106**, 1766-1771.